SUPPLEMENTARY MATERIALS FOR

Impact of drought on isoprene fluxes assessed using field data, satellite-based GLEAM soil moisture and HCHO observations from OMI

Beata Opacka [1,*], Jean-François Müller [1], Trissevgeni Stavrakou [1], Diego G. Miralles [2], Akash Koppa [2], Brianna R. Pagán [2,3], Mark J. Potosnak [4], Roger Seco [5], Isabelle De Smedt [1] and Alex B. Guenther [6]

[1] Royal Belgian Institute for Space Aeronomy (BISA), Avenue Circulaire 3, 1180 Brussels, Belgium; jfm@aeronomie.be (J.F.M.); jenny@aeronomy.be (T.S.); isabelle.desmedt@aeronomie.be (I.D.S);
[2] Hydro-Climate Extremes Lab (H-CEL), Department of Environment, Ghent University, Coupure Links 653, 9000 Ghent, Belgium; Diego.Miralles@UGent.be (D.G.M.); akash.koppa@ugent.be (A.K.); Brianna.Pagan@UGent.be (B.R.P.)
[3] Remote Sensing, SpacesenseAI, rue Jean-Jacques Rousseau 62, 75001 Paris, France
[4] Environmental Science and Studies, DePaul University, 1110 W Belden Ave., Chicago, IL 60614, USA; mark.potosnak@depaul.edu
[5] Institute of Environmental Assessment and Water Research (IDAEA-CSIC), Carrer Jordi Girona 18-26, 08034 Barcelona, Catalonia, Spain; email@rogerseco.cat
[6] Department of Earth System Science, University of California Irvine, 3216 Croul Hall, Irvine, CA 92697-3100, USA; alex.guenther@uci.edu

* *Correspondence to*: Beata Opacka (beata.opacka@aeronomie.be)

Contents

1. Leaf area index at the MOFLUX site

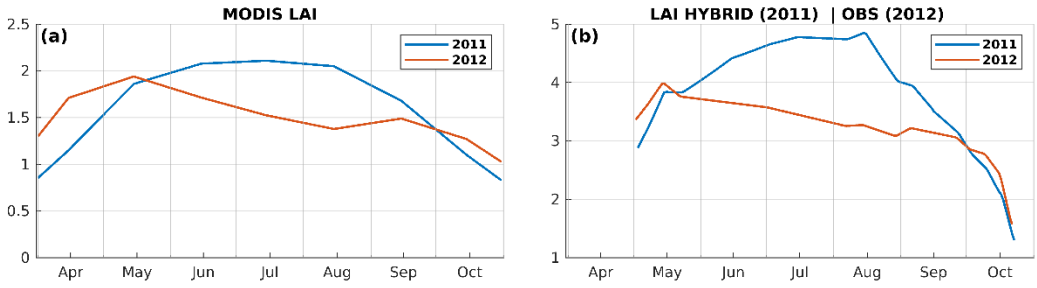

Figure S1: Comparison of LAI at the MOFLUX from (**a**) monthly MODIS dataset and (**b**) daily hybrid (obtained combining MODIS and observed LAIs) and observed.

2. Temporal frequency for the analysis of isoprene and HCHO columns at MOFLUX

Figure S2 (a) shows the daily number of OMI HCHO data within a 20-km radius of the MOFLUX site. The other panels of Figure S2 show the (b) weekly averaged, (c) biweekly averaged, and (d) monthly averaged OMI HCHO columns. Daily and weekly averaged columns do not provide enough valid data points to conduct meaningful analysis. We consider here as valid the column averages that exceed the detection limit calculated as $3\left(\frac{\sigma_r}{\sqrt{N}}\right) \times 1.6$, with σ_r, the random retrieval error and N, the number of data contributing to the average. The evaluation of TROPOMI HCHO data against ground-based measurements indicate that the random TROPOMI uncertainties are underestimated by about a factor 1.6 ([109]). Given the similarities between the OMI and TROPOMI retrievals, a similar underestimation is expected for OMI data. As seen in Figure S2, after screening out columns below the detection limit, we are left with about 5 (4) % and 62 (31) % of valid data in year 2011 (2012) for daily and weekly OMI HCHO columns, respectively. More than 70% of bi-weekly averages are above the detection limit in both years.

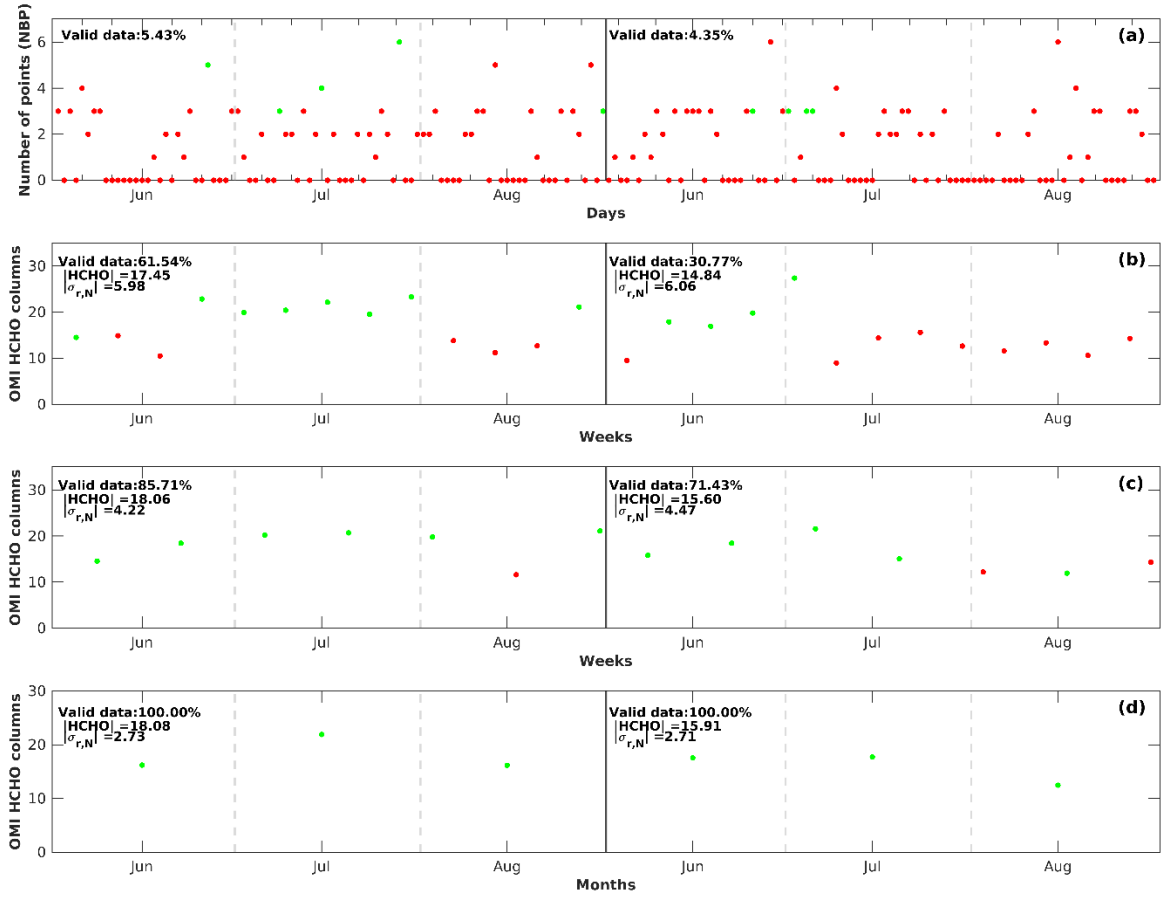

Figure S2: **(a)** Number of daily OMI data above detection limit within a 20-km radius of the MOFLUX site during summers 2011/2012, and HCHO columns averaged **(b)** weekly (7 days), **(c)** biweekly (14 days) and **(d)** monthly. Valid points (averaged columns above the detection limit, defined in text) are shown in green, whereas non valid points are marked in red. Mean of averaged HCHO columns ($|HCHO|$) over the entire summer months and random retrieval error divided by the square root of the number of data points N ($|\sigma_{r,N}|$) are given inset.

3. Difference in maximal temperature and PAR over 2011 and 2012

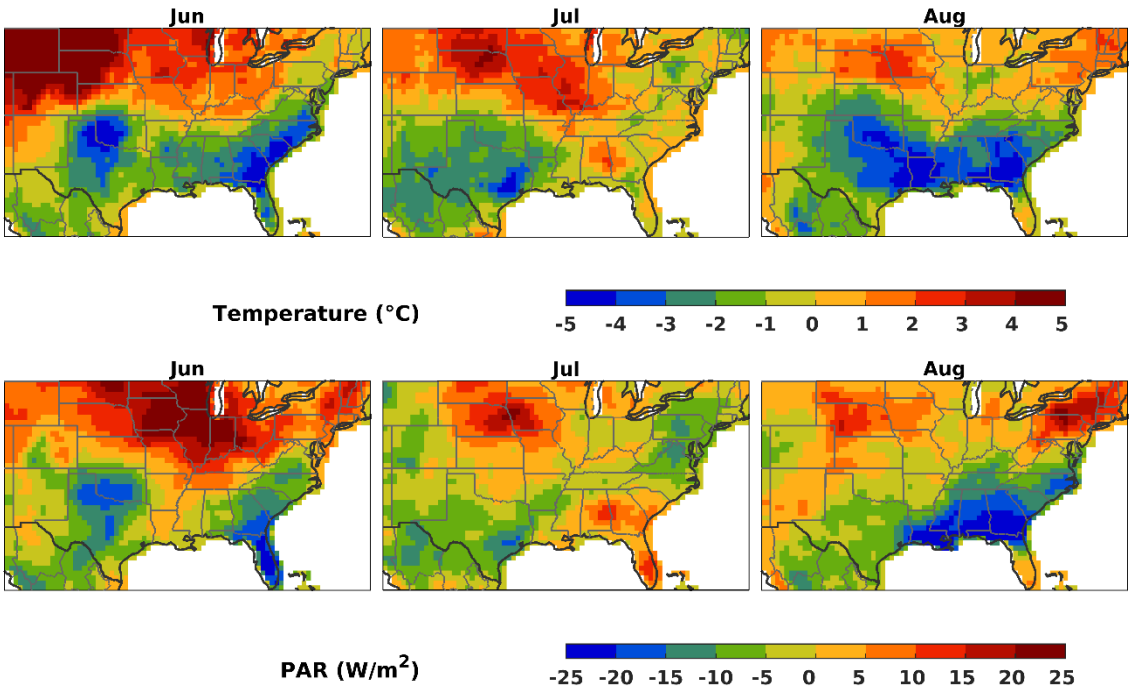

Figure S3: Absolute difference (2012 – 2011) in monthly maximum temperature (in °C) (top panel) and PAR (in W/m²) (bottom panel).

4. Distribution of the MEGANv2.1. drought activity factor over eastern U.S.

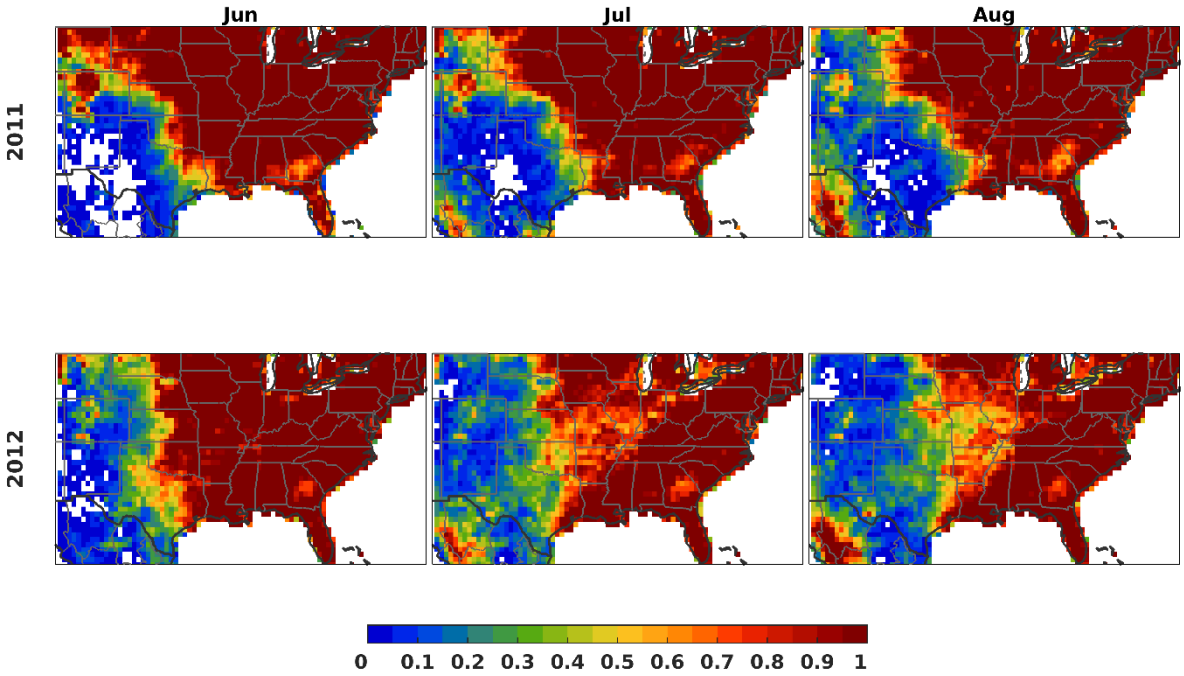

Figure S4: Monthly soil moisture stress factor γ_{SM}^{OPT} (Equation 2) using GLEAM soil moisture and the optimized parameter $\Delta\theta = 0.12$ for June-July-August 2011 (top row) and 2012 (bottom row).

5. Sensitivity of OMI HCHO columns to the radius around the MOFLUX site

Table S1: Sensitivity of OMI HCHO column to the choice of the radius around the MOFLUX site.

	June			July			August		
	2011	**2012**	**RC**	**2011**	**2012**	**RC**	**2011**	**2012**	**RC**
OMI HCHO (10 km)	16.2	13.7	***-16%***	19.0	16.5	***-13%***	15.6	14.4	***-8%***
OMI HCHO (20 km)	16.2	17.5	***+8%***	21.9	17.7	***-13%***	16.2	12.5	***-23%***
OMI HCHO (30 km)	16.2	16.1	***-1%***	21.6	19.8	***-9%***	15.2	12.4	***-18%***

6. Screening of OMI columns for effects of fires and aerosols

Pyrogenic sources are a minor source of HCHO at the global scale but can be of importance in the vicinity of fires. Furthermore, biomass burning generate aerosols which might disrupt the OMI HCHO retrieval and potentially impair the comparisons. These effects warrant some caution. Therefore, we conducted an additional analysis aiming to minimize the potential impact of aerosols and biomass burning emissions on the model comparisons with OMI HCHO data. More precisely, in this analysis, (1) we exclude OMI data (and the corresponding model data) affected by strong local pyrogenic emissions according to the GFED4s inventory, by excluding data for which the daily carbon flux exceeds 5×10^{12} molec.cm^{-2}, and (2) we exclude OMI data impacted by biomass burning (and other pollution) plumes, by requiring that the daily Aerosol Optical Depth (AOD) from the Copernicus Atmospheric Monitoring System (CAMS) should not exceed 0.4 (Section 2.6). The AOD threshold value is chosen in order to keep a good coverage of monthly-averaged OMI observations over the main BVOC source regions, while limiting potential contamination by pyrogenic or anthropogenic pollution plumes. Moreover, we also mitigate the potential impact of aerosols on the OMI HCHO retrieval.

After the screening, the number of OMI measurements available every month over the U.S. decreases (see Figure S5), in particular in the SEUS region (by about 30%). Over the TX region (8% decrease), the effect on the spatial distribution of differences in HCHO columns is marginal. After application of this screening, the observed and modelled HCHO column differences are displayed in Figure S6 and Table S2. We find that the filtering impacts mainly the spatial distribution in the southeast U.S., without changing the conclusions (Table S2). The TX region was marginally affected by the filtering. The OMI data filtering has also minimal impact on the conclusions of the global model analysis (Figure S8).

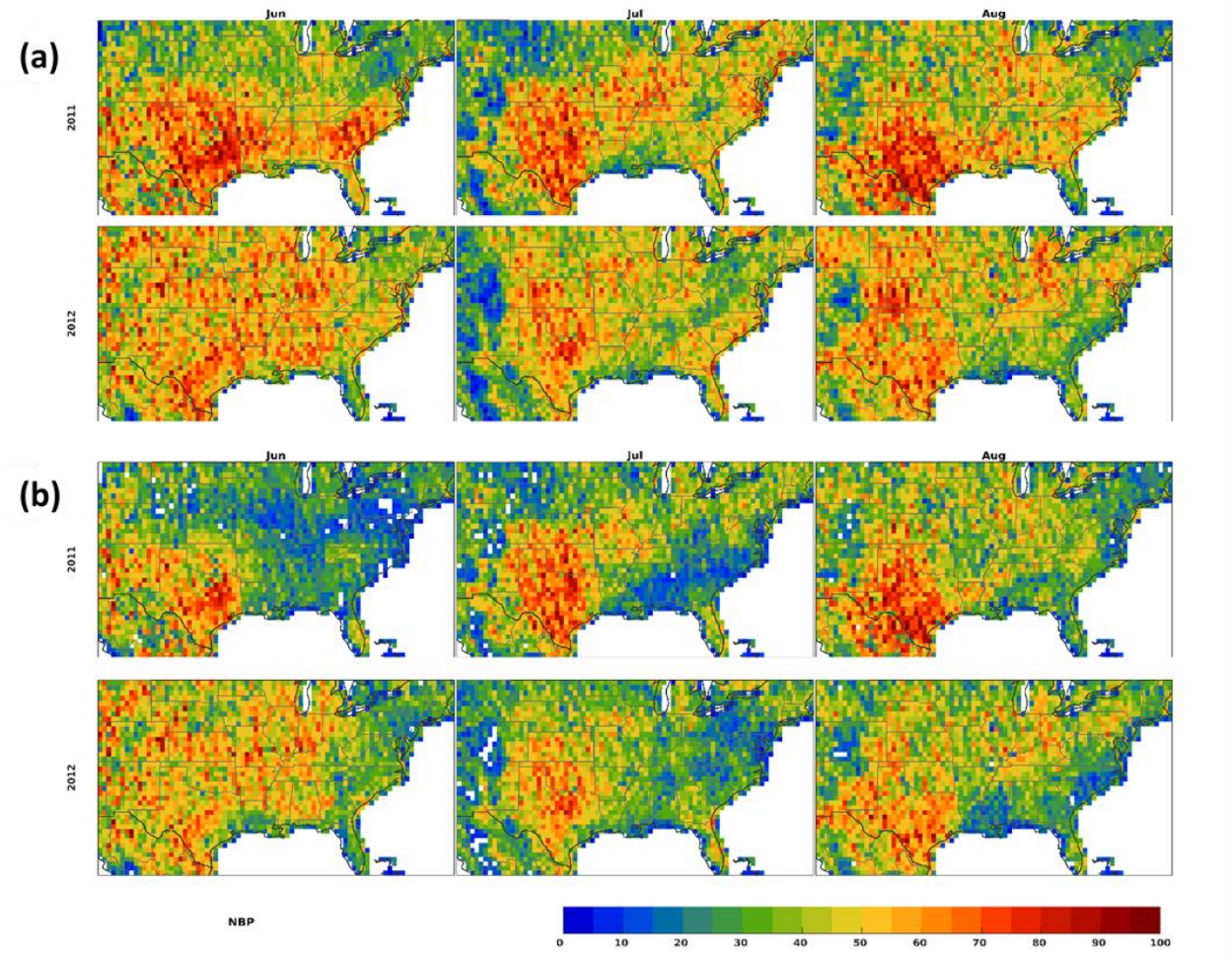

Figure S5: Spatial distribution of number of OMI HCHO observations per pixel during each summer month in 2011/2012 **(a)** in the original dataset and **(b)** in the filtered dataset.

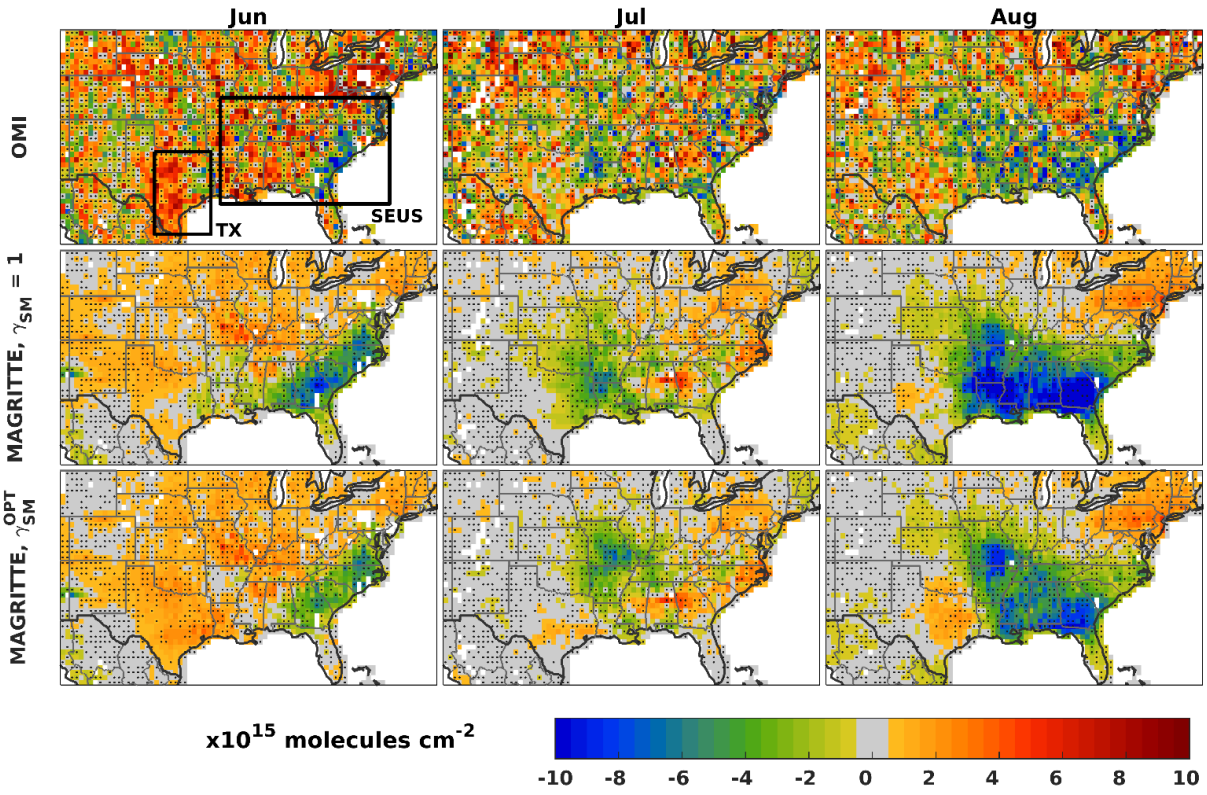

Figure S6: As Figure 6, when excluding OMI data with high AOD or high biomass burning fluxes.

Table S2: As in Table 2, when excluding OMI data with high AOD or high biomass burning fluxes.

		OMI			MAGRITTE, $\gamma_{SM} = 1$			MAGRITTE, γ_{SM}^{OPT}		
		June	**July**	**August**	**June**	**July**	**August**	**June**	**July**	**August**
TX	**2011**	10.6	12.8	13.8	13.3	14.4	17.6	10.7	11.2	12.2
	2012	13.0	12.5	13.6	13.5	13.0	15.6	12.1	11.4	12.6
	RC (%)	**+23 (±23)**	**-2 (±18)**	**-1 (±17)**	**+2**	**-10**	**-11**	**+13**	**+1**	**+4**
SEUS	**2011**	14.3	16.2	15.9	17.9	19.8	21.2	16.4	18.2	18.7
	2012	15.0	15.7	13.5	16.8	19.3	15.9	16.2	17.7	14.6
	RC (%)	**+5 (±18)**	**-3 (±17)**	**-15 (±18)**	**-6**	**-2**	**-25**	**-1**	**-3**	**-22**

7. Global correlation coefficients with OMI HCHO columns

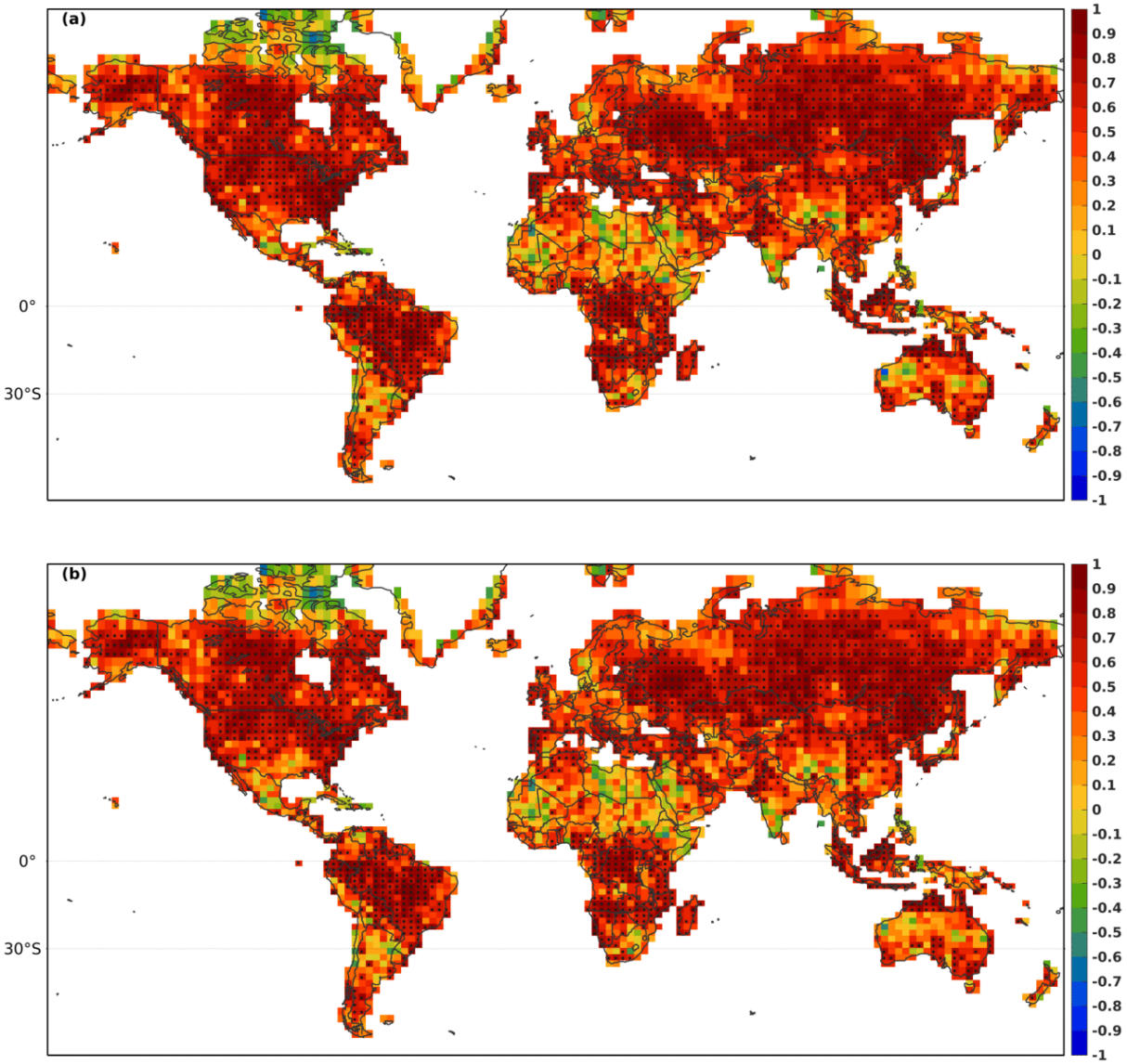

Figure S7: Pearson coefficient of correlation between the observed evolution of seasonally averaged HCHO columns during 2005—2016 and the model-calculated values for (**a**) IMAGES, $\gamma_{SM}^{0.04}$ (with $\Delta\theta$ = 0.04) and (**b**) IMAGES, γ_{SM}^{OPT}. The seasonal averages are calculated over the months of June-August in the Northern Hemisphere (>0°N), February-April in the 0-30° S latitudinal band, and December-February below the 30th parallel. The stippling represents the statistically significant correlation coefficient ($p<0.05$).

8. Impact of revised drought stress factor on OMI/model correlation, after application of OMI filtering

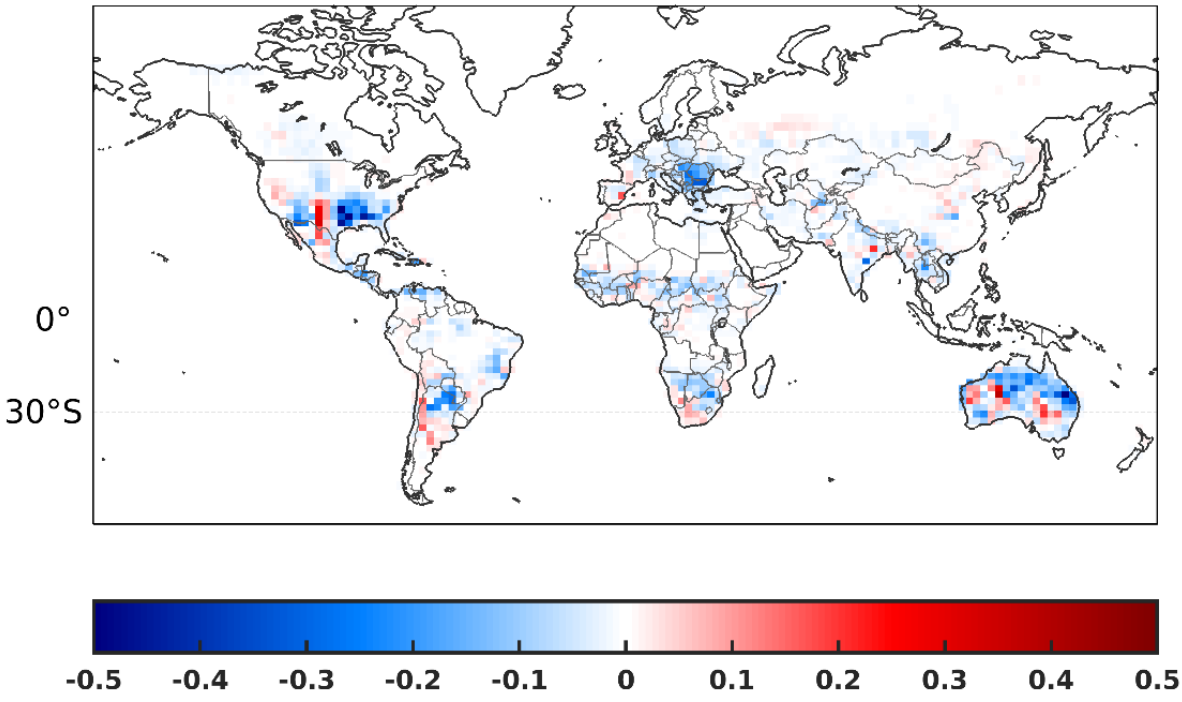

Figure S7: As Figure 7, but with OMI data filtered for high AOD and high pyrogenic fluxes.